Lessons on Conditional Gene Targeting in Mouse Adipose Tissue

Lessons on Conditional Gene Targeting in Mouse Adipose Tissue

Kevin Y. Lee,[1] Steven J. Russell,[1] Siegfried Ussar,[1] Jeremie Boucher,[1] Cecile Vernochet,[1] Marcelo A. Mori,[1] Graham Smyth,[1] Michael Rourk,[1] Carly Cederquist,[1] Evan D. Rosen,[2] Barbara B. Kahn,[2] and C. Ronald Kahn[1]

Conditional gene targeting has been extensively used for in vivo analysis of gene function in adipocyte cell biology but often with debate over the tissue specificity and the efficacy of inactivation. To directly compare the specificity and efficacy of different Cre lines in mediating adipocyte specific recombination, transgenic Cre lines driven by the adipocyte protein 2 (aP2) and adiponectin (Adipoq) gene promoters, as well as a tamoxifen-inducible Cre driven by the aP2 gene promoter (iaP2), were bred to the Rosa26R (R26R) reporter. All three Cre lines demonstrated recombination in the brown and white fat pads. Using different floxed loci, the individual Cre lines displayed a range of efficacy to Cre-mediated recombination that ranged from no observable recombination to complete recombination within the fat. The Adipoq-Cre exhibited no observable recombination in any other tissues examined, whereas both aP2-Cre lines resulted in recombination in endothelial cells of the heart and nonendothelial, nonmyocyte cells in the skeletal muscle. In addition, the aP2-Cre line can lead to germline recombination of floxed alleles in ~2% of spermatozoa. Thus, different "adipocyte-specific" Cre lines display different degrees of efficiency and specificity, illustrating important differences that must be taken into account in their use for studying adipose biology. ***Diabetes*** **62:864–874, 2013**

Adipose tissue plays an important role in metabolism through its storage and release of triglycerides, peptide hormones (adipokines) and other proteins, and in the case of brown fat, for its role in thermogenesis (1). Excess adipose tissue (i.e., obesity) is a risk factor for numerous comorbidities, including type 2 diabetes, coronary heart disease, hypertension, hepatosteatosis, and even cancer (2).

Analysis of adipocyte function in vivo has benefited from the development of mouse lines that use the Cre/LoxP site-specific recombination system to inactivate specific genes in fat (3). The use of such targeting systems has allowed researchers to clarify the relative contribution of the adipose tissue in many metabolic phenotypes and circumvent lethality that might be associated with inactivation of genes at the whole-body level. Several different Cre transgenes have been used for this purpose. The most common use the promoter of the mouse adipocyte protein-2 (aP2) gene, which encodes fatty acid-binding protein-4 (Fabp4). A 5.4-kb piece of the aP2 promoter/enhancer has been shown to be sufficient to direct expression in adipocytes (4,5). At least three independent laboratories have developed aP2-Cre transgenic mice. The first aP2-Cre line was created by Kleanthis Xanthopoulos (6); subsequently, the aP2-Cre^{BI} line was created by Barbara Kahn (Beth Israel, Boston, MA) (7), and the aP2-Cre^{SI} was created by Ronald Evans (Salk Institute, San Diego, CA) (8). In addition, the aP2 promoter has been used by the Chambon laboratory (Institut de Génétique et Biologie Moléculaire et Cellulaire, Paris, France) to drive the expression of a tamoxifen-inducible Cre transgene (aP2-CreERT2), which is only able to recombine floxed alleles in the presence of 4-hydroxytamoxifen (4-OHT) (9,10).

Although aP2/Fabp4 was originally identified as an adipocyte-specific protein, recent studies have shown that Fabp4 is also expressed in other cell types (11), including macrophages (12–14), the lymphatic system (15), and during embryogenesis (16). To circumvent the possible side effects of gene deletion of the aP2-Cre in tissues other than adipocytes, two laboratories have developed adiponectin-Cre transgenic mice (Adipoq-Cre), with expression of a Cre recombinase driven by the promoter/regulatory regions of the mouse adiponectin locus using a bacterial artificial chromosome (BAC) transgene (17) or by a 5.4-kB promoter fragment (18).

In the current study, we have directly compared the specificity and efficacy of three mouse transgenic Cre lines—the aP2-Cre^{BI}, aP2-CreERT2, and Adipoq-Cre BAC transgenic mouse lines—in mediating adipocyte-specific recombination using a number of different floxed alleles as well as by breeding these mice to the LacZ-Gt(ROSA)26Sor^{tm1Sor} (termed R26R-lacZ) reporter mouse, in which Cre-mediated recombination irreversibly activates a lacZ reporter gene (19). We find that all of the Cre lines induce recombination in the adipose tissue. In addition, the aP2-Cre^{BI} and aP2-CreERT2 lines both induce recombination in the capillary endothelium in the heart and in intermyofibrillar cells in the skeletal muscle, but not in macrophages in adipose tissue. Interestingly, we find that different floxed gene loci display differential sensitivity to Cre-mediated recombination and that different adipose depots recombine to different extents. The aP2-Cre^{BI} can also lead to germline recombination of floxed alleles. These results illustrate the differences between "adipose-specific" Cre lines and caveats in their use that are critical for interpretation of research using these models.

RESEARCH DESIGN AND METHODS

Animals and diets. aP2-Cre^{BI} and aP2-CreERT2 mice were maintained on a C57BL/6 background. Adipoq-Cre mice had also been backcrossed to

From the [1]Section on Integrative Physiology and Metabolism, Joslin Diabetes Center, Harvard Medical School, Boston, Massachusetts, and the [2]Division of Endocrinology, Beth Israel Deaconess Medical Center, Boston, Massachusetts.

Corresponding author: C. Ronald Kahn, c.ronald.kahn@joslin.harvard.edu.

Received 16 August 2012 and accepted 2 December 2012.

DOI: 10.2337/db12-1089

This article contains Supplementary Data online at http://diabetes.diabetesjournals.org/lookup/suppl/doi:10.2337/db12-1089/-/DC1.

C57BL/6; however, single nucleotide polymorphism panel analysis revealed that these mice, although largely C57BL/6, still have markers of a mixed genetic background (http://jaxmice.jax.org/strain/010803.html).

The Cre mice were bred to Gt(ROSA)26Sor^{tm1Sor} obtained from Jackson Laboratories on the C57BL/6 background. Mice with floxed alleles of insulin receptor (*IR*), *Hif1β*, *Igf1r*, *Dicer*, *Shox2*, and *Tfam* have previously been described (20–25), as have the generation of fat-specific knockouts of *Glut4*, peroxisome proliferator-activated receptor-γ (*Pparγ*), *IR*, *Hif1β*, *Tfam*, and *IR*/*Igf1r* with the aP2-Cre mouse (7,26–30). The generation of fat-specific knockouts of *PTP1B*, *Ppar-γ* coactivator-1α (*Pgc1α*), and SH2-containing protein tyrosine phosphatase-2 (*Shp2*) with the Adipoq-Cre have also been described (31–33). All mice were housed in a mouse facility on a 12-h light/dark cycle in a temperature-controlled room with ad libitum access to water and food.

For tamoxifen treatment of aP2-CreERT2, tamoxifen was dissolved in a solution of 10% ethanol in sunflower seed oil at a concentration of 50 mg/mL. Mice were gavaged with this solution (100 μL) daily for 5 days and killed 2 weeks later. Daily gavage with 4-hydroxytamoxifen (4-OHT) led to a slight decrease (~3 g) in the body weight of mice. Similar recombination efficiencies, without effects on body weight, were observed after three cycles of gavage every other day and killing the animals 2 weeks after the last dose. Longer treatment protocols did not increase deletion efficacy. Other treatment methods led to undesirable complications. Intraperitoneal injection 4-OHT led to excess oil unabsorbed in the abdomen and mild peritonitis, and subcutaneous injection led to the formation of granulomas at the site of injection (data not shown).

Animal care and study protocols were approved by the Joslin Diabetes Center Animal Care Committee and were in accordance with the National Institutes of Health guidelines.

Detection of β-galactosidase activity. Fat pads were whole-mount stained. Other tissues were cut into 10-μm cryosections and stained for β-galactosidase activity, as previously described (34).

Macrophage isolation. Peritoneal macrophages were collected by injecting 5 mL ice-cold PBS supplemented with 1% BSA into the peritoneal cavity and collecting the resultant cell suspension. Fat resident and recruited macrophages were collected by excising and mincing epididymal white adipose tissue into 5 mL with Liberase Thermolysin Medium (21.5 μg/mL, *Dicer* Roche) and incubated at 37°C for 45 min with shaking. Larger particles were removed using 250-μm nylon sieves and the filtrates were centrifuged at 300*g* for 5 min to separate floating adipocytes from the stromal-vascular fraction (SVF) pellets. SVF pellets containing macrophages and cell suspensions containing peritoneal macrophages were treated with 100 μL ACK lysis buffer (Lonza) for 5 min at room temperature, and washed with PBS. Macrophages were stained in 100 μL staining buffer (PBS containing 1% BSA with F4/80-APC; E-Bioscience). Cells were again washed, filtered through a 40-μm mesh, and F4/80-positive cells were sorted by FACSAria (BD Biosciences).

Immunofluorescence and immunohistochemistry. Colocalization of Fabp4 and CD31 was assessed in the fat by whole-mount immunofluorescence using hamster anti-mouse CD31 monoclonal antibodies (1:500; BD Biosciences) and rabbit anti-Fabp4 polyclonal antibodies (1:200; Cell Signaling), anti-hamster-FITC (1:1,000; BD Biosciences), and goat anti-rabbit Alexa 564 (1:1,000; Invitrogen). Photographs were generated using an inverted confocal microscope. Colocalization in heart and muscle was assessed using cryosections with the same antibodies. F4/80 localization was assessed using rat anti-F4/80 (1:100; Abcam) and goat anti-rat Alexa 488 (1:1000; Invitrogen).

Quantification of β-galactosidase activity. Total protein lysates were made by homogenizing tissue in M-PER Reagent (Pierce). Five hundred micrograms of concentrated protein lysate was added to 100 μL β-galactosidase

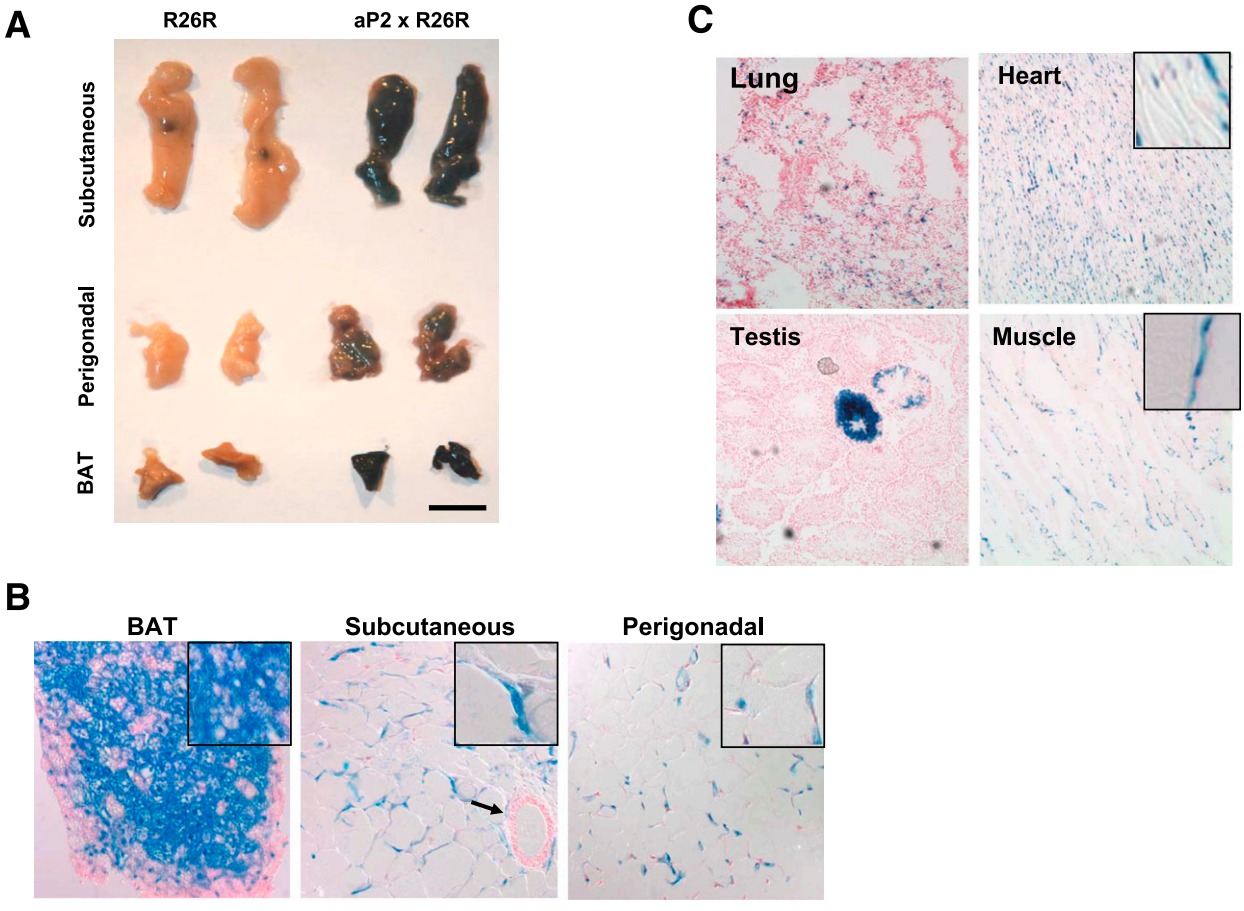

FIG. 1. Analysis of Cre-induced recombination in the aP2-Cre^{BI} R26R-lacZ Mice. *A*: Whole-mount X-gal staining of fat pads from the aP2-Cre^{BI} R26R-lacZ mouse. Brown, subcutaneous, and perigonadal adipose tissue from 3-month-old chow-fed aP2-Cre^{BI} R26R-lacZ (n = 4) after overnight incubation in X-gal staining solution (scale bar = 1 cm). *B*: Representative sections from aP2-Cre^{BI} R26R-lacZ X-gal stained fat pads. Fat pads from panel *A* were fixed in Bouin's fixative and embedded in paraffin; 8-μm sections were hematoxylin stained. Representative images are shown. *C*: Representative sections from aP2-Cre^{BI} R26R-lacZ tissues stained with X-gal. Lung, heart, testis, and muscle from 3-month-old chow-fed aP2-Cre^{BI} R26R-lacZ (n = 4) were embedded in optimal cutting temperature medium; 10-μm sections were X-gal stained, and counterstained with nuclear fast red. Representative images are shown.

staining solution (34) and incubated overnight. Absorbance was measured at 635 nmol/L.

Assessment of germline recombination. DNA from tail biopsies was extracted and subjected to PCR. In addition to primers that discriminate between floxed and wild-type alleles, an additional primer to assess the presence of recombined floxed alleles (Δ allele) was added. For the IR locus: forward primer 5′-ctgaatagctgagaccacag-3′; reverse primer 5′- gatgtgcaccccatgtctg-3′; delta primer 5′-tctatcaaccgtgcctagag-3′. For the Tfam locus: forward primer 5′-ctgccttcctctagcccggg-3′; reverse primer 5′-gtaacagcagacaacttgtg-3′; delta primer 5′-ctctgaagcacatggtca at-3′.

RESULTS

aP2-Cre^{BI} recombination in adipose tissue, heart, skeletal muscle, and testis. aP2-Cre^{BI} mice were bred with R26R-lacZ reporter mice to visualize the tissues in which Cre-mediated recombination occurred. X-gal staining of fat pads of 3-month-old mice, revealed strong recombination in the brown adipose tissue (BAT), subcutaneous fat, and perigonadal fat (Fig. 1*A*). Sections from these fat pads show extensive lacZ staining in adipocytes but no staining in large blood vessels in the subcutaneous fat, as indicated by the arrows (Fig. 1*B*). This staining was relatively fat-specific, because no staining, or only scattered rare blue nuclei, were observed in other tissues, including the liver, kidney, brain, thymus, adrenal, pancreas, spleen, uterus, ovary, skin, and salivary gland (Supplementary Fig. 1). However, X-gal staining was observed in the heart, lung, and selected nuclei in skeletal muscle (Fig. 1*C*). Strikingly, strong recombination was also observed in the developing spermatogonium of ~2% of the seminiferous tubules but was completely absent in the other 98% (Fig. 1*C*, lower left), suggesting clonal germ line recombination occurs during spermatogenesis.

Localization of endogenous Fabp4 expression. When crossed with R26R-lacZ reporter mice, aP2-Cre^{BI} mice show recombination limited mostly to the fat pads, but also in the heart and muscle. Quantitative (q)PCR analysis of *Fabp4* and *Adiponectin* mRNA across a wide panel of tissues revealed that both are primarily expressed in fat, with very low expression levels in other tissues (Supplementary Fig, 2). To better define these additional cell types exhibiting recombination in the aP2-Cre^{BI} mice, we localized endogenous aP2/Fabp4 in mouse adipose tissue,

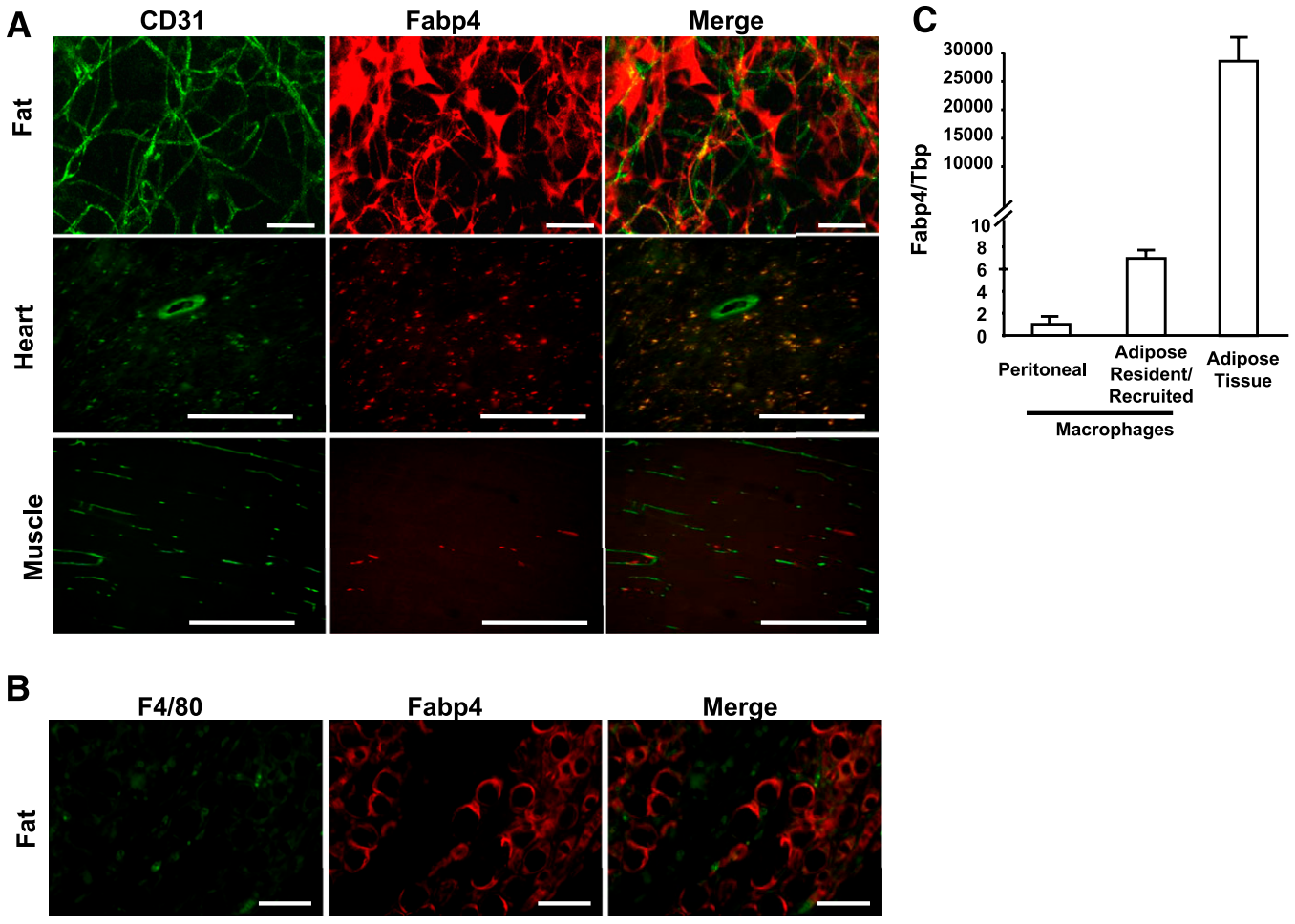

FIG. 2. Endogenous expression of Fabp4 in wild-type mice. ***A*****: Double immunofluorescence for the endothelial cell markers CD31 and Fabp4 in the perigonadal fat, heart, and muscle of 2-month-old C57BL/6 male mice. Perigonadal fat pads were whole-mount stained and representative composite (original magnification ×10) pictures created from Z-stacks of several images taken by confocal microscopy are shown (scale bar = 50 μm). Images for double immunofluorescence for CD31 and Fabp4 in heart and muscle are representative original magnification ×20 images (scale bar = 200 μm).** ***B*****: Double immunofluorescence for the macrophage marker, F4/80 and Fabp4 in the perigonadal fat of wild-type mice. Representative images (original magnification ×40) of double immunofluorescence for F4/80 and Fabp4 in the perigonadal fat of 12-month-old wild-type C57BL/6 mice (scale bar = 50 μm).** ***C*****: qPCR analysis of *Fabp4* from sorted F4/80-positive cells from the peritoneal cavity and adipose tissue and whole adipose tissue of male mice (*n* = 6) after 12 weeks of a high-fat diet (started at age 6 weeks). Data are normalized to the expression of TATA binding protein (Tbp) and are shown as mean ± SEM.**

myocardium, and skeletal muscle by double immunofluorescence with anti-Fabp4 and anti-CD31, which stains endothelial cells, or an anti-F4/80 antibody, which marks macrophages (Fig. 2*A*). Confocal images of the whole-mount stained perigonadal adipose tissue demonstrated only very slight colocalization of CD31 and Fabp4 (Fig. 2*A*). No colocalization was observed between anti-F4/80 and anti-Fabp4 antibodies in perigonadal fat (Fig. 2*B*), demonstrating that Fabp4 is not highly expressed in macrophages or endothelial cells. The immunofluorescence demonstrates that Fabp4 expression is limited almost exclusively to adipocytes. Furthermore, qPCR analysis of sorted F4/80 positive macrophages from the peritoneal fluid and perigonadal adipose tissue shows that levels of *Fabp4* in macrophages are several thousandfold lower than those found in whole adipose tissue (Fig. 2*C*).

Colocalization of CD31 and Fabp4 was not observed in skeletal muscle; however, in the heart, Fabp4 did colocalize with CD31 staining in small capillaries. Interestingly, large CD31-positive blood vessels in the heart did not stain positively for Fabp4, indicating that endogenous Fabp4 is expressed only in a specific subset of endothelial cells (Fig. 2*A*).

aP2-CreERT2 recombination in adipose tissue, heart, muscle, and salivary gland. The 4-OHT–inducible Cre driven by the aP2 promoter (aP2-CreERT2) allows for temporal control of recombination (9). In the absence of 4-OHT, no X-gal staining was observed in any tissue in male or female mice (Fig. 3*A* and *C*, Supplementary Fig. 3). Upon oral 4-OHT treatment, X-gal staining was observed in the subcutaneous and perigonadal fat pads (Fig. 3*A*). Sections through these fat pads show limited X-gal staining (Fig. 3*B*). In agreement with observations from the aP2-Cre^{BI}, recombination was observed in capillaries of the myocardium and in interfibrillar cells in skeletal muscle (Fig. 3*C*). Unlike the aP2-Cre^{BI}, recombination was also observed in the epithelium of the salivary gland after 4-OHT exposure (Fig. 3C). No staining was observed in any other tissue after 4-OHT treatment (Supplementary Fig. 4).

Adipoq-Cre recombination in adipose tissue. Whole-mount X-gal staining of fat pads of 6-week-old Adipoq-Cre mice crossed to R26R-lacZ reporter mice revealed strong recombination in the brown, subcutaneous, and perigonadal fat (Fig. 4*A*). Upon sectioning, robust lacZ staining can be seen in adipocytes from all depots, with no staining in the blood vessels of the subcutaneous fat (Fig. 4*B*, arrows). The recombination from the Adipoq-Cre mice was fat-specific, because absolutely no staining was observed in other tissues, including the liver, kidney, brain, thymus, adrenal, pancreas, spleen, lung, testis, salivary gland, ovary, or uterus (Supplementary Fig. 5). In contrast to the aP2-Cre^{BI} lines, no expression was observed in the myocardium or skeletal muscle; however, some recombination was observed in dermal adipocytes of the skin (Fig. 4*C*).

Quantification of Cre expression and recombination of the aP2-Cre^{BI}, aP2-CreERT2, and Adipoq-Cre lines. Cre mRNA levels from subcutaneous, perigonadal, and brown fat, as well as muscle, heart, and liver, were analyzed in aP2-Cre^{BI}, aP2-CreERT2, and Adipoq-Cre mice using qPCR. In all three fat pads, the aP2-Cre^{BI} exhibited the highest Cre expression at the mRNA level, with expression also observed in the heart and muscle (Fig. 5*A*). The aP2-CreERT2 expressed low levels of Cre mRNA in the fat pads and also exhibited expression in the heart and liver. Conversely, in the Adipoq-Cre mice, Cre mRNA

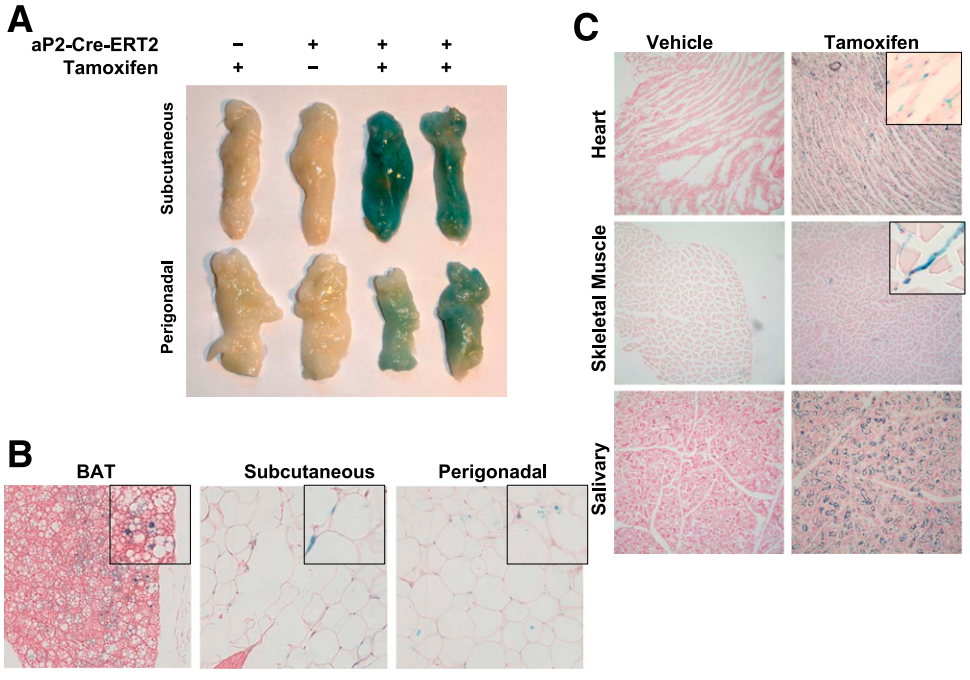

FIG. 3. Analysis of Cre-induced Recombination in the aP2-CreERT2 R26R-lacZ mice. *A*: Whole-mount X-gal staining of fat pads from the aP2-CreERT2 R26R-lacZ mouse. Subcutaneous and perigonadal adipose tissue from 4 month old chow-fed aP2-CreERT2 R26R-lacZ (n = 3 per group) treated with vehicle or tamoxifen after overnight incubation in X-gal staining solution. *B*: Representative sections from aP2-CreERT2 R26R-lacZ X-gal-stained fat pads. Fat pads from Fig. 2*A* were fixed in Bouin's fixative, embedded in paraffin, and 8-μm sections were stained with hematoxylin. Representative images are shown. *C*: Representative sections from aP2-CreERT2 R26R-lacZ tissues stained with X-gal. Heart, skeletal muscle, and salivary from 4-month-old chow-fed aP2-CreERT2 R26R-lacZ treated with vehicle or tamoxifen (n = 3) were embedded in optimal cutting temperature medium, and 10-μm sections were X-gal stained and counterstained with nuclear fast red. Representative images are shown.

expression was found exclusively in the fat pads, with no detectable expression in heart, muscle, or liver. Assessment of Cre protein level by Western blot showed that in the subcutaneous and brown fat, Cre protein levels were high both in the aP2-Cre^{BI} and Adipoq-Cre, with only minimal expression in the aP2-CreERT2 (Fig. 5*B*).

Whole-mount β-galactosidase staining demonstrated that the aP2-Cre^{BI} and Adipoq-Cre mouse lines effectively recombine the Rosa locus. However, to quantify this recombination, a colorimetric assay was developed using β-galactosidase activity as a readout for the degree of recombination of tissues from aP2-Cre^{BI} and Adipoq-Cre lines crossed to the R26R-lacZ reporter mice. Lysates from R26R-lacZ reporter mice alone were used to establish baseline readings. β-Galactosidase activity was found in all fat pads of aP2-Cre^{BI} and Adipoq-Cre mice. aP2-Cre^{BI} Cre showed a greater extent of recombination in BAT, whereas Adipoq-Cre showed slightly greater recombination in the subcutaneous fat and perigonadal fat. A small amount of β-galactosidase activity over background was observed in the aP2-Cre^{BI} in the heart and muscle, but not in liver (Fig. 5*C*).

Recombination efficiency of the aP2-Cre^{BI} is allele- and age-dependent. The aP2-Cre^{BI} mouse has been crossed to multiple lines harboring different floxed alleles to generate fat-specific knockout mouse models. In most cases, recombination was adipose-specific as determined by qPCR analysis, which showed no significant recombination in the liver, heart, or brain with any of the floxed alleles. Interestingly, in some cohorts, up to a 60% reduction of *IR* mRNA was observed in the skeletal muscle of fat-specific insulin receptor knockout (FIRKO) animals, but this was not observed with any of the other genes (Table 1). There was also differential recombination efficiency across different alleles and in different fat pads. This may represent differences in efficacy of recombination or differential expression of the targeted locus in different cells within the fat pad. qPCR analysis showed reductions of *Hif1β* RNA of 63, 68, and 89% in whole fat perigonadal, subcutaneous, and brown fat compared with floxed controls. In the white fat depots, the lower recombination rate was at least partly due to the presence of *Hif1β* in other cells of the fat pad. Thus, qPCR analysis of isolated adipocytes revealed 83 and 86% reduction of *Hif1β* mRNA in perigonadal and subcutaneous adipocytes, respectively. There was also modest reduction of *Hif1β* in the SVF of the perigonadal and subcutaneous fat of 27 and 40%, suggesting recombination in preadipocytes or early adipocytes present in the fraction.

Recombination of *Shox2* in aP2-Cre^{BI} mice resulted in reductions of *Shox2* mRNA of 48, 58, and 81% in perigonadal, subcutaneous, and brown fat compared with floxed controls, respectively. Recombination of the Pparγ locus was also very efficient with the aP2-Cre^{BI} mice. Fat-specific ablation of *Pparγ* with the aP2-Cre^{BI} led to a complete absence of *Pparγ* mRNA in brown fat. In the white fat pads, mRNA *Pparγ* levels were reduced more than 90% in the subcutaneous white fat and completely ablated in the perigonadal fat pad.

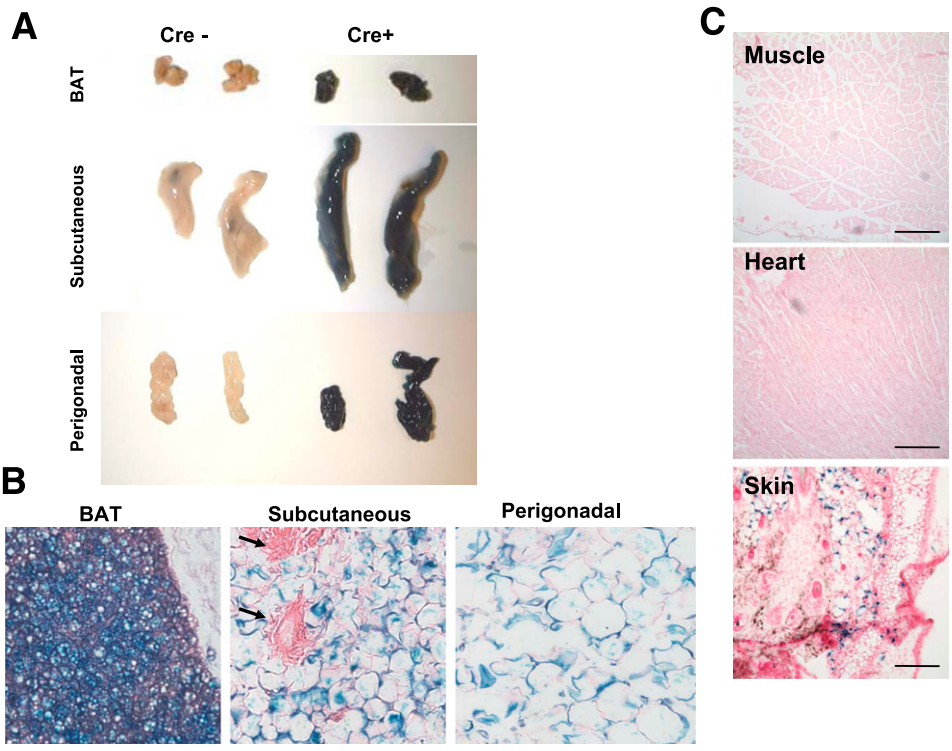

FIG. 4. Analysis of Cre-induced recombination in the Adipoq-Cre R26R-lacZ mice. *A*: Whole-mount X-gal staining of fat pads from the Adipoq-Cre R26R-lacZ mouse. Brown, subcutaneous, and perigonadal adipose tissue from 6-week-old chow-fed R26R-lacZ only or Adipoq-Cre R26R-lacZ (n = 4 per group) after overnight incubation in X-gal staining solution. *B*: Representative sections from Adipoq-Cre R26R-lacZ fat pads stained with X-gal. Fat pads from Fig. 2*A* were fixed in Bouin's fixative, embedded in paraffin, and 8-μm sections were stained with hematoxylin. Representative images are shown. Arrows indicate negative staining in the vasculature. *C*: Representative sections from Adipoq-Cre R26R-lacZ tissues stained with X-gal. Muscle, heart, and skin from 3-month-old chow-fed Adipoq-Cre R26R-lacZ were embedded in optimal cutting temperature compound, and 10-μm sections were stained with X-gal and counterstained with nuclear fast red. Blue staining in skin section is due to the presence of dermal adipocytes. Representative images are shown.

TABLE 1
RNA expression (ratio of mRNA expression to floxed controls)

Mouse	Cre line	Ref	Age/sex (month)	Gene	Whole fat pads			Isolated adipocytes		SVF		Other tissues			
					PG	SC	Brown	PG	SC	PG	SC	Liver	Muscle	Heart	Brain
FIRKO	aP2-Cre^{BI}		2/♂	*IR*	0.69 ± 0.14	0.65 ± 0.15	0.21 ± 0.03*					1.16 ± 0.11	0.40 ± 0.04*	1.01 ± 0.03	1.05 ± 0.03
			7/♂	*IR*	0.34 ± 0.03*	0.36 ± 0.01*	0.12 ± 0.02*	0.42 ± 0.05				0.73 ± 0.06	0.43 ± 0.04*	1.13 ± 0.11	1.07 ± 0.05
FIGIRKO	aP2-Cre^{BI}	30	4/♂	*IR*	0.66 ± 0.26	0.40 ± 0.13*	0.48 ± 0.07*	0.59 ± 0.14	0.63 ± 0.02*	0.81 ± 0.12	0.98 ± 0.13	0.90 ± 0.05	0.84 ± 0.06		1.02 ± 0.03
			12/♂	*IR*	0.46 ± 0.14*	0.38 ± 0.06*	0.44 ± 0.06*	0.59 ± 0.06*	0.66 ± 0.06	0.77 ± 0.08	0.63 ± 0.16				
			4/♂	*IGF1R*	0.67 ± 0.13	0.65 ± 0.10	0.59 ± 0.33	0.54 ± 0.13*	0.65 ± 0.09*	0.80 ± 0.11	0.77 ± 0.13	1.13 ± 0.12	0.96 ± 0.24		
			12/♂	*IGF1R*	0.64 ± 0.11*	0.68 ± 0.02*	0.74 ± 0.11	0.61 ± 0.04*	0.66 ± 0.09*	0.79 ± 0.08	0.93 ± 0.08			0.83 ± 0.18	
F-Pparγ-KO	aP2-Cre^{BI}	26	4–5	*Pparγ*	ND	~0.10	No tissue					~2.0			
F-HIF1βKO	aP2-Cre^{BI}	38	2/♀	*Hif1β*	0.37 ± 0.13*	0.32 ± 0.10*	0.11 ± 0.03*	0.17 ± 0.07*	0.14 ± 0.05*	0.73 ± 0.11	0.60 ± 0.13*	1.21 ± 0.12	0.87 ± 0.14	0.97 ± 0.09	
F-Shox2KO	aP2-Cre^{BI}		3/♀	*Shox2*	0.52 ± 0.19	0.42 ± 0.18*	0.19 ± 0.03*	0.37 ± 0.10*	0.22 ± 0.06*			0.52 ± 0.26		1.06 ± 0.11	
F-TFKO	aP2-Cre^{BI}	29	5/♂	*Tfam*	0.98 ± 0.16	0.81 ± 0.05	0.33 ± 0.19	1.69 ± 0.29	0.46 ± 0.15	1.05 ± 0.25	0.90 ± 0.20	1.06 ± 0.32	0.96 ± 0.08	0.94 ± 0.05	
F-DicerKO	aP2-Cre^{BI}		NA	*Dicer*	Early postnatal lethality										
iFIRKO	aP2-CreERT2		2/♂	*IR*	0.57 ± 0.09	0.67 ± 0.07	0.67 ± 0.08								
iF-DicerKO	aP2-CreERT2		3/♂	*Dicer*	0.86 ± 0.03	0.46 ± 0.06*	0.51 ± 0.07*	0.67 ± 0.26	0.94 ± 0.01						
adF-TFKO	Adipoq-Cre		4/♂	*Tfam*	1.03 ± 0.41	1.13 ± 0.06	0.27 ± 0.19*	0.25 ± 0.11*	0.51 ± 0.14*	1.32 ± 0.32	0.92 ± 0.26				
adF-DicerKO	Adipoq-Cre		3/♂	*Dicer*	0.30 ± 0.07*	0.39 ± 0.17*	0.19 ± 0.01*	0.39 ± 0.08*	0.26 ± 0.01*	0.67 ± 0.12	1.11 ± 0.18				
adF-PgcIαKO	Adipoq-Cre	31		*Pgc1a*	<0.20	<0.20	<0.10	<0.10				NC	NC		

Recombination efficiency as assessed by qPCR of fat specific knockout mouse models in fat, isolated adipocytes, the stromal vascular fraction of fat, and other tissues of different floxed alleles. All animals were maintained on a chow diet, and data are represented as a ratio of mRNA expression compared with floxed controls ± SEM. FIRKO (n = 6–7), FIGIRKO (n = 5), F-TFKO (n = 5), F-Hif1βKO (n = 4), F-Shox2KO (n = 4), iFIRKO (n = 4), iF-DicerKO (n = 4), adF-TFKO (n = 4), adF-DicerKO (n = 3). NC, not changed; ND, not detectable; N/A, not applicable; PG, perigonadal; SC, subcutaneous. *Significant difference ($P < 0.05$).

FIG. 5. Quantification of Cre expression and recombination of the aP2-Cre^{BI}, aP2-CreERT2, and Adipoq-Cre lines. *A*: Quantification of Cre mRNA expression of tissues from aP2-Cre^{BI}, aP2-CreERT2, and Adipoq-Cre lines. qPCR analysis of subcutaneous (SC) fat, perigonadal (PG) fat, brown fat, muscle, heart, and liver was performed using tissues from 3- to 5-month-old aP2-Cre^{BI} (n = 4), aP2-CreERT2 (n = 4), and Adipoq-Cre (n = 3) mice. All animals were maintained on a chow diet, and data are represented as mean ± SEM. *B*: Quantification of Cre protein expression of adipose tissues from aP2-Cre^{BI}, aP2-CreERT2, and Adipoq-Cre mice. Western blot analysis of subcutaneous, perigonadal, and brown fat from 3- to 5-month-old aP2-Cre^{BI}, aP2-CreERT2, and Adipoq-Cre mice. All animals were maintained on a chow diet. *C*: Quantification of recombination in tissues from aP2-Cre^{BI} and Adipoq-Cre mice. A colorimetric assay for β-galactosidase activity was performed on subcutaneous fat, perigonadal fat, brown fat, muscle, heart, and liver from control R26R-lacZ mice (n = 3), aP2-Cre^{BI} R26R-lacZ (n = 3), and Adipoq-Cre R26R-lacZ (n = 2) mice. All animals were 4 to 6 months old and maintained on a chow diet. Data are represented mean ± SEM.

Conversely, using the aP2-Cre^{BI} line and mice with a floxed *Tfam* (mitochondrial transcription factor A) allele, there was a 67% reduction at the mRNA level in the brown fat, but no significant reduction of *Tfam* mRNA was observed in the perigonadal or subcutaneous fat pads. When the fat pads were digested, there was a significant 54% reduction of *Tfam* mRNA in the isolated subcutaneous adipocytes, but no reduction in isolated perigonadal adipocytes, demonstrating a major depot-specific difference in recombination. No differences in *Tfam* mRNA levels were observed in the isolated SVF of these mice.

In contrast to the other gene knockouts presented here, which were born at expected Mendelian ratios, attempts to ablate Dicer using the aP2-Cre^{BI} resulted in early postnatal lethality precluding further analysis. This early postnatal lethal phenotype was also observed by another group that

TABLE 2
Protein expression (ratio of protein expression to floxed controls)

Mouse	Cre line	Ref	Age/sex (month)	Protein	Whole fat pads			Isolated adipocytes	SVF	Other tissues			
					PG	SC	Brown			Liver	Muscle	Heart	Brain
F-HIF1βKO	aP2-CreBI	36	N/A	Hif1β	~0.50	N/A	N/A	~0.1	0.60–0.70[a]	NC	NC		
Hif1α	aP2-CreBI	36	N/A	Hif1α	~0.50	N/A	~0.50	~0.12	NC	NC	NC		
FIRKO	aP2-CreBI	27	3	IR	ND	ND	ND	0.01–0.15[e]	N/A	NC	NC	NC	NC
F-Glut4KO	aP2-CreBI	7	2–12 ♀/♂	Glut4	0.01–0.30	0.01–0.30	0.01–0.30	N/A[b]	N/A[b]		NC	NC	
F-PTP1B-KO	aP2-CreBI			PTP1B	~0.50								NC
adF-Glut4KO	Adipoq-Cre		2–3	Glut4	0.01–0.20	0.01–0.20	<0.01	N/A[b]	N/A[b]		NC	NC	
adF-PTP1B$^{-/-}$	Adipoq-Cre	32		PTP1B	<0.20[c]	<0.20[c]	<0.10[c]	ND	NC	NC	NC		
adF-SHKO	Adipoq-Cre	33		Shp2	~0.30		Decreased	~0.15	NC	NC	NC		
adF-Pgc1αKO	Adipoq-Cre	31		Pgc1α	ND[d]		ND[d]						

Recombination efficiency as assessed by Western blot of fat-specific knockout mouse models in fat, isolated adipocytes, the SVF of fat, and other tissues of different floxed alleles. All animals were maintained on chow diet, and data are represented as a ratio of protein expression compared with floxed controls. N/A, not applicable; NC, not changed; ND, not detectable; PG, perigonadal, SC, subcutaneous. [a]Macrophage expression. [b]Glut4 is only expressed in adipocytes, and not in other cell types in the adipose tissue. [c]Estimation. [d]No induction during chronic cold exposure. [e]Mice were selected for efficient IR recombination.

used the alternate aP2-Cre^{SI} (35) but was not observed with the Adipoq-Cre (see below), indicating that this is due to an inactivation of Dicer in some nonadipose tissue.

qPCR analysis also showed that *IR* at the mRNA level was reduced by 79% in brown fat compared with floxed controls in the fat pads of 2-month-old FIRKO animals but was not significantly reduced in the perigonadal and subcutaneous fat. The recombination efficiency of the *IR* locus increased with age. By age 7 months, FIRKO animals had reductions of *IR* mRNA of 66, 64, and 88% in perigonadal, subcutaneous, and brown fat compared with floxed controls. Similarly, in the double fat-specific knockout of insulin-like growth factor 1 receptor (IGF1R) and IR (FIGIRKO) animals, recombination efficiency of the *IR* locus was also improved in the perigonadal fat pad from a 34% to a 54% reduction from 4 to 12 months but not in the BAT or subcutaneous fat pad. No change in recombination efficiency of *IGF1R* was observed between 4- and 12-month-old animals. Thus, these data demonstrate recombination efficiency of the aP2-Cre^{BI} can vary across both alleles and fat depots, and in certain contexts, the recombination efficiency may also vary across the age of the mice.

The varying degree of recombination efficiency, as measured by mRNA message levels, was also observed when protein concentrations were measured by Western blotting. IR was not detectable at the protein level in FIRKO fat pads and was 85–99% reduced in isolated adipocytes (27). Likewise, Glut4 protein was significantly reduced by 70–99% after recombination with the aP2-Cre^{BI} (7). In agreement with the mRNA levels, in adipocytes isolated from F-Hif1αKO and F-Hif1βKO mice, protein levels of Hif1α and Hif1β are reduced ~90% by the aP2-Cre^{BI} (36). Conversely, protein levels of PTP1B were only reduced by ~50% in perigonadal fat pads of F-PTP1BKO mice. These data further confirm the allele-dependent recombination efficiency of the aP2-Cre^{BI} (Table 2).

Less efficient recombination is observed with the aP2-CreERT2. The aP2-CreERT2 has been used to effectively ablate genes such as the retinoid X receptor α (*Rxrα*) and *Pparγ* in the adipose tissue (9,37). qPCR analysis showed aP2-CreERT2 reduced *IR* at the mRNA level 43, 33, and 33% in perigonadal, subcutaneous, and brown fat tissue compared with floxed controls. Thus, recombination of the *IR* locus was less efficient in the inducible knockout compared with the constitutive knockouts with the aP2-Cre^{BI} (Table 1). The inducible fat-specific DicerKO resulted in 54 and 49% decreases of *Dicer* mRNA in the whole subcutaneous adipose tissue and BAT, with no significant difference in the perigonadal fat.

Efficient recombination is achieved with the Adipoq-Cre across numerous alleles. Owing to the poor recombination of the floxed *Tfam* and protein tyrosine phosphatase 1B (*PTP1B*) alleles using the aP2-Cre^{BI} and the early lethality it caused in floxed *Dicer* mice, we crossed these mice to the Adiponectin-Cre mouse. All mice lines were born at expected Mendelian ratio. As with the aP2-Cre, significant ablation of *Tfam* from whole fat pads at the mRNA level was only observed with the Adipoq-Cre in the brown fat, with a 73% reduction, but no significant reduction was observed in the perigonadal or subcutaneous fat pads (Table 1). This reflects the high levels of *Tfam* in nonadipocyte cells in the fat pad because isolated adipocytes from perigonadal and subcutaneous fat show significant 75 and 49% reductions of *Tfam* mRNA (Table 1). Western blot analysis of PTP-1B demonstrates

efficient ablation with the Adipoq-Cre in whole fat pads, with reductions of 80–90%. In addition, PTP-1B protein was undetectable in isolated adipocytes, but no change was seen in the SVF of fat pads, the liver, or the muscle (Table 2) (21). Efficient ablation by the Adipoq-Cre was also observed with *Dicer*, with reductions of *Dicer* mRNA of 70, 61, and 81% in whole perigonadal, subcutaneous, and brown fat compared with floxed controls. Similar reductions of *Dicer* mRNA was also observed in isolated adipocytes, with 61 and 74% reduction of *Dicer* mRNA in perigonadal and subcutaneous adipocytes, respectively, with no significant reductions in the SVFs of perigonadal or subcutaneous fat. Efficient ablation using the Adipoq-Cre mouse has also been reported for the floxed alleles of *Pgc1α*, and *Shp2* (31,33). qPCR analysis showed Adipoq-Cre reduced *Pgc1α* RNA more than 80% in the perigonadal and subcutaneous fat, and more than 90% in brown fat. A >90% reduction of *Pgc1α* RNA was found in perigonadal adipocytes, with no changes in expression in the liver or the muscle (Table 1). Similarly, no Pgc1α protein was detectable even after chronic cold exposure (Table 2). These data demonstrate specific and efficient recombination of multiple alleles in adipocytes using the Adipoq-Cre mice.

Incidence of germline deletion when using the aP2-Cre^{BI}. Mice harboring Cre transgenes have been shown to lead to occasional germline recombination of floxed alleles (38). Because recombination is observed in testis of aP2-Cre^{BI} mice, we tested our mice lines for evidence of germline recombination. A PCR-based assessment of recombination was developed for each floxed allele and performed with isolated tail DNA. For the *IR* locus, a 280-bp amplified product indicates a wild-type exon 4, a 320-bp product represents an intact floxed exon 4, and a 220-bp product represents a floxed allele after Cre-mediated recombination. The recombined allele is termed the delta (Δ) allele (Fig. 6*A*). A similar PCR strategy was developed for *Tfam* in which a 350-bp product indicates a wild-type allele, a 420-bp product represents an intact *Tfam* allele with exon 6 and 7 floxed, and a 300-bp product represents the Δ*Tfam* allele created by Cre-mediated recombination (Fig. 6*B*). No evidence of germline recombination was found with the aP2-CreERT2 (mated before tamoxifen induction) or Adipoq-Cre mouse lines. However, Cre-mediated excision of floxed transgene occurs in a number of mice upon crossing with the aP2-Cre^{BI} line. The Δ allele, was detectable in the tail DNA, in the absence of any cell previously demonstrated to express aP2, and

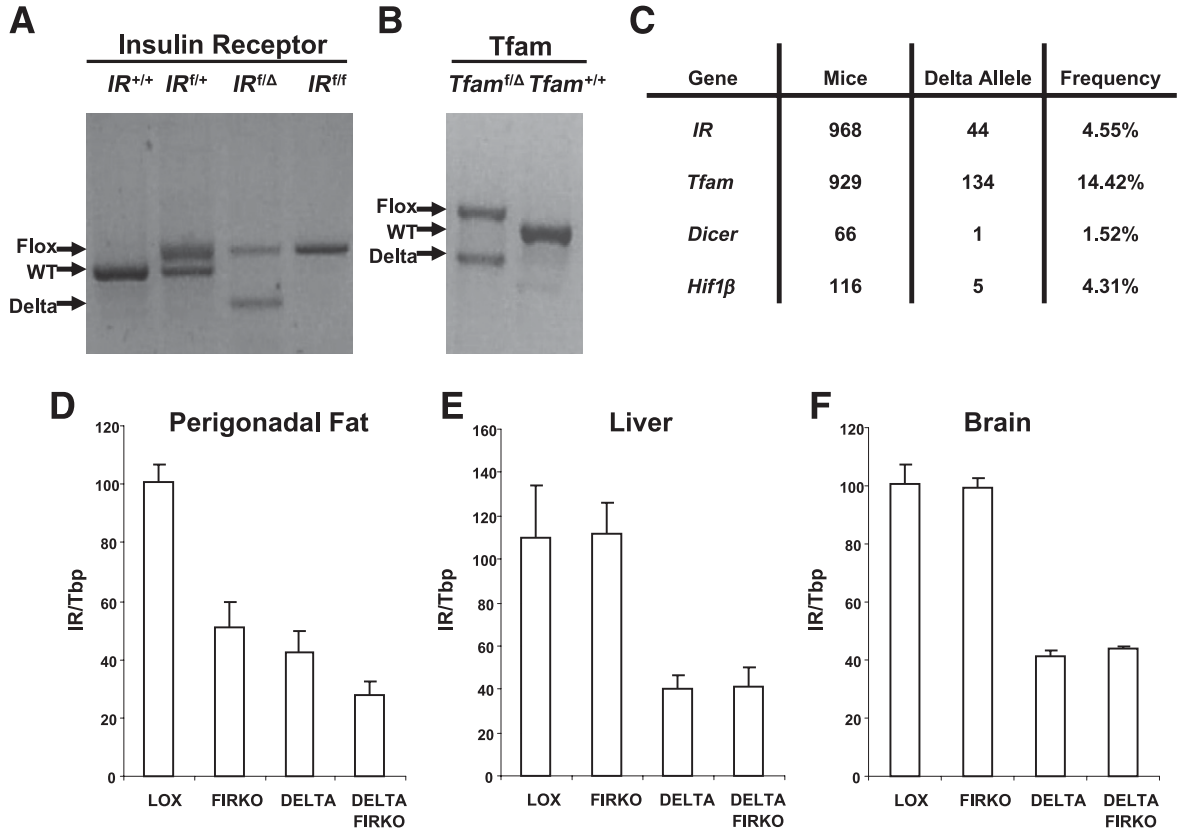

FIG. 6. Germline deletion of floxed alleles when using the aP2-Cre^{BI}. *A*: Evidence of recombination of the *IR* locus from the aP2-Cre^{BI} in DNA from mouse tails. DNA was extracted from tails of progeny of the aP2-Cre^{BI} mouse and mice with the floxed *IR*. The recombination status of the IR locus (from left to right) are *IR*$^{+/+}$, *IR*$^{fl/+}$, *IR*$^{fl/\Delta}$, and *IR*$^{fl/fl}$. WT, wild-type. *B*: Evidence of recombination of the *Tfam* locus with the aP2-Cre^{BI} in DNA from mouse tails. DNA was extracted from tails of progeny of the aP2-Cre^{BI} mouse and mice with a floxed *Tfam* locus. The recombination status of the *Tfam* locus (from left to right) are *Tfam*$^{fl/\Delta}$ and *Tfam*$^{+/+}$. *C*: Frequency of the Δ allele is illustrated in progeny of the aP2-Cre^{BI} mouse and mice with floxed alleles of *IR*, *Tfam*, *Dicer*, and *Hif1β*. *D*: Expression of *IR* was compared using qPCR in perigonadal fat of 3-month-old male *IR*$^{fl/fl}$ (LOX), aP2-Cre^{BI} *IR*$^{fl/fl}$ (FIRKO), *IR*$^{fl/\Delta}$ (DELTA), or aP2-Cre^{BI} *IR*$^{fl/\Delta}$ (DELTA FIRKO) mice. Data are normalized to the expression of *Tbp* and are shown as mean ± SEM of six to seven samples. *E*: Expression of *IR* was compared using qPCR in the liver of 3-month-old male animals as in panel *D*. Data are normalized to the expression of *Tbp* and are shown as mean ± SEM of six to seven samples. *F*: Expression of *IR* was compared using qPCR in the brain of 3-month-old male animals as in panel *D*. Data are normalized to the expression of *Tbp* and are shown as mean ± SEM of six to seven samples.

the incidence of the Δ allele varies across floxed transgenes, from as low as 1.6% in *IR*-floxed animals to as high as 14.4% in *Tfam*-floxed animals (Fig. 6C). Furthermore, qPCR analysis of *IR* mRNA from tissues of animals possessing a Δ *IR* allele, shows that the presence of the Δ allele, independently of the presence of the aP2-Cre transgene, leads to an ~60% loss of expression in perigonadal fat, as well as liver and brain (Fig. 6*D–F*). These results indicate that the aP2-Cre^{BI} line can lead to germline recombination of the floxed alleles, resulting in whole-body heterozygous knockout mice.

DISCUSSION

During the past 2 decades, advances in the use of site-specific recombinases have added greatly to our ability to manipulate cells and gene expression. These site-specific recombinases bind to and recombine specific sequences of DNA, allowing researchers to heritably label cells, conditionally inactivate or activate genes, and even ablate cells based on their gene expression. Thus far, studies examining the in vivo role of specific genes in adipocytes by conditional ablation have largely relied on the adipose-specific expression of the aP2 promoter (4,5), with (9,10) or without (7,8) additional regulation by tamoxifen. Recently, Adipoq-Cre lines were created as a possible alternative model to conditionally ablate genes in adipose tissue (17,18). More than 70 published reports have relied upon aP2-Cre or Adipoq-Cre lines, and although several caveats in their use have been alluded to, thus far, these have not been systematically assessed. In the current study, we have performed a direct comparison and analysis of these fat-specific Cre lines.

The tissue and cell-type specificity of these different mouse transgenic Cre lines was determined by crossing them to the R26R-lacZ reporter mouse and analyzing the tissues from the resultant mice for recombination. Of the three Cre lines analyzed in this study, the Adipoq-Cre showed the most specific expression in white and brown fat. The aP2-Cre^{BI} R26R-lacZ mice and the aP2-CreERT2 R26R-lacZ mice also showed recombination both in brown and white fat; however, there was nonadipose expression with both aP2-Cre lines. This included expression in the capillaries of the myocardium and in perivascular cells in the skeletal muscle. On the one hand, that two independent aP2-Cre mouse lines gave similar patterns suggests that the recombination in these tissues is due to eutopic expression of Cre recombinase directed by the aP2 promoter. On the other hand, the differences between the aP2-CreERT2 and aP2-Cre^{BI} mice, including the staining within the testis and salivary gland, may be due to the different sites of transgene integration.

The large degree of recombination in the endothelial cells of the heart observed in the aP2-Cre^{BI} and the aP2-Cre^{SI} may explain why fat-specific Dicer-knockout animals created with aP2-Cre exhibit perinatal lethality due to Dicer's known roles in vessel formation and maintenance (39). However, such cell-type specific loss of gene expression in a tissue of mixed cell types, such as the heart or skeletal muscle, may be difficult to detect by qPCR or Western blot because the other cells in the tissue continue normal expression. Likewise, stochastic recombination in the germ cell lines would be difficult to detect without histological analysis. It is also worth noting that the endogenous Fabp4 expression is observed only in the small capillaries and not in the large vessels of the heart. This specific expression in a distinct subset of endothelial cells suggests developmental differences between endothelial cells. Some studies of the FIRKO mouse have observed a reduction of IR gene expression in skeletal muscle. However, because this reduction is only observed in the FIRKO, this effect may be a secondary effect specific to this line and not due to aP2-Cre deletion.

Although previous reports have shown Fabp4 expression in many other tissues, including the kidney, liver, and skin (11), little or no recombination is observed in the aP2-Cre lines in any of these tissues. The levels of Fabp4 are very low in nonadipose tissue, and the lack of recombination in these tissues may be due to low levels of Cre expression that are below the threshold needed for recombination. Alternatively, the enhancer regions needed for expression in these tissues may be missing from the aP2 promoter fragment used to generate these Cre mice. Previous reports have also shown that *Fabp4* is expressed in macrophages (40) within the heart. Here, we demonstrate that macrophages within the adipose tissue do not express significant levels of Fabp4. These findings are confirmed by the absence of recombination that we observe in the macrophages of the aP2-Cre^{BI}.

In addition to differences among the Cre mice, we demonstrate that the different floxed gene loci display a range of sensitivity to recombination when using these different Cre lines. With the aP2-Cre^{BI}, very efficient recombination was observed in the *Hif1β*, *Shox2*, *Glut4*, and *IR* loci, with far less recombination found in the combination of the *IR/IGF1R* double knockout loci and the *PTP1B* and *Tfam* locus. Several factors may contribute to this range of sensitivity to Cre-mediated recombination. First, different floxed alleles are known to have differential sensitivity to Cre-mediated recombination, with some loci inherently more difficult to recombine (41). Another potential factor that may confound these results is that some of the genes being inactivated may be necessary for adipogenesis or survival. Work from in vitro models demonstrates that ablation of Hif1β (28), Shox2 (unpublished data), or Glut4 (7) does not affect adipogenesis or cellular survival. Similarly, differentiation of preadipocytes that lack IR can be compensated for by expression of IGF1R (30). On the other hand, Dicer appears to be indispensible for adipogenesis (42), and combined loss of IR and IGF1R results in complete failure of adipocyte differentiation (30). Although cells with a knockdown of Tfam differentiate into adipocytes (43) ablation of Tfam leads to increased apoptosis (44–46). Thus, in models that ablate genes necessary for adipogenesis or cellular survival, recombination would appears to be less efficient because the knockout adipocytes never develop. Conversely, genes that are expressed exclusively in the mature adipocytes, including *Glut4* (47) and *Pparγ* (48), would have a greater recombination efficiency than those expressed in multiple cell types.

Within the FIRKO animals, we also find that there is an age-dependent increase in recombination efficiency. Several factors may be contributing to the improved recombination. First, as animals age, the cellular composition of the fat pads may shift, including a decrease of preadipocytes (49). This would lead to a relative increase in the proportion of adipocytes compared with other cells, and because the aP2-Cre is active in adipocytes, recombination efficiency would appear to be improved. In addition, transcriptional activity and changes in splicing from the *IR* locus have been observed during aging (50),

suggesting that epigenetic modifications to the *IR* locus occur with age. It is possible that these changes in the *IR* locus may change its susceptibility to Cre-mediated recombination.

Cre mRNA levels in the fat pads of aP2-Cre^{BI} mice are higher than in the aP2-CreERT2 or Adipoq-Cre mice. Because the same 5.4-kb promoter fragment was used in the creation of the aP2-Cre^{BI} and aP2-CreERT2 lines, the difference in expression between these two lines is most likely due to differential copy number or to different sites of transgene integration. Conversely, because only one to two copies of a BAC transgene integrate into the genome, the levels of Cre transgene observed in the Adipoq-Cre mice most likely reflect the high endogenous expression of Adipoq mRNA. Despite the lower Cre expression level, the Adipoq-Cre mice demonstrate slightly greater recombination in both the subcutaneous and perigonadal fat. These results suggest that the greater Cre expression in the aP2-Cre^{BI} fat is due to higher expression of Cre per cell and not to a greater number of cells expressing Cre. In fact, the greater recombination efficiency observed in the Rosa locus, as well as in the *Tfam*, *Dicer*, and *PTP1B* loci, suggests that the Adipoq-Cre may direct Cre expression to a more complete population of adipocytes than the aP2-Cre^{BI}.

Finally, we have shown that transmission of the aP2-Cre^{BI} can lead to germline deletion (Δ) of floxed alleles. The incidence of Δ alleles varies across floxed transgenes and leads to a reduction of gene expression. Strong staining and specific LacZ staining could be seen in ~2% of seminiferous tubules of aP2-Cre^{BI} R26R-lacZ testis, leading to populations of recombined spermatid precursors. Because within individual mice the Δ allele can be independent of the presence of Cre, recombination in the germ cells most likely occurs early in spermatogenesis, thus allowing Cre and Δ alleles to segregate during meiosis. Although we did not observe oocytes with lacZ staining, the Δ allele can also arise when the female is the carrier of the Cre transgene, suggesting that germline recombination may also occur in the oocyte. In our studies of using the aP2-Cre, we excluded all animals carrying the Δ allele from further analysis or breeding. However, if such mice are not excluded from the breeding strategy, the Δ allele leads to whole-body heterozygous knockouts in the next generation. This needs to be assessed in all mice made using Cre-Lox recombination because it can lead to misleading phenotypes if not recognized. Although we have not directly studied the aP2-Cre^{SI} mouse, we believe this may account for the striking difference in recombination specificity between original publication (8) and the subsequent analyses (http://cre.jax.org/Fabp4/Fabp4-creNano.html) (51), which found widespread recombination.

In conclusion, in this study we have analyzed the efficacy and specificity of transgenic Cre lines driven by the aP2 and adiponectin gene promoters. All three lines we examined demonstrated recombination in fat with minimal staining in most other tissues. The aP2-Cre line demonstrates both an allele- and age-dependent sensitivity to Cre-mediated recombination within the fat. Finally, we show that the aP2-Cre line can lead to germline recombination of floxed alleles. These results are the first systematic analysis of these Cre lines that have been widely used to study adipocyte biology and highlight important considerations and implications not only in their use but also in the need for careful characterization of Cre lines in general.

ACKNOWLEDGMENTS

This work was supported by a Joslin Training Grant (T32DK-007260) to K.Y.L., a Human Frontier Sciences Program Long-term Fellowship to S.U., and National Institutes of Health Grants DK-60837 and-DK 82655, an American Diabetes Association Mentor-Based Award, and the Mary K. Iacocca Professorship to C.R.K.

No potential conflicts of interest relevant to this article were reported.

K.Y.L. researched data and wrote the manuscript. S.J.R., S.U., J.B., C.V., M.A.M., G.S., M.R., and C.C. researched data. E.R. contributed to discussion and reviewed and edited the manuscript. B.B.K. researched data, contributed to discussion, and reviewed and edited the manuscript. C.R.K. contributed to discussion and wrote the manuscript. C.R.K. is the guarantor of this work, and, as such, had full access to all the data in the study and takes responsibility for the integrity of the data and the accuracy of the data analysis.

The authors thank Chris Cahill of the Joslin Advanced Microscopy Core, and the Joslin Flow Cytometry Core for technical assistance.

REFERENCES

1. Tseng YH, Cypess AM, Kahn CR. Cellular bioenergetics as a target for obesity therapy. Nat Rev Drug Discov 2010;9:465–482
2. Abelson P, Kennedy D. The obesity epidemic. Science 2004;304:1413
3. Branda CS, Dymecki SM. Talking about a revolution: the impact of site-specific recombinases on genetic analyses in mice. Dev Cell 2004; 6:7–28
4. Graves RA, Tontonoz P, Platt KA, Ross SR, Spiegelman BM. Identification of a fat cell enhancer: analysis of requirements for adipose tissue-specific gene expression. J Cell Biochem 1992;49:219–224
5. Ross SR, Graves RA, Greenstein A, et al. A fat-specific enhancer is the primary determinant of gene expression for adipocyte P2 in vivo. Proc Natl Acad Sci U S A 1990;87:9590–9594
6. Barlow C, Schroeder M, Lekstrom-Himes J, et al. Targeted expression of Cre recombinase to adipose tissue of transgenic mice directs adipose-specific excision of loxP-flanked gene segments. Nucleic Acids Res 1997; 25:2543–2545
7. Abel ED, Peroni O, Kim JK, et al. Adipose-selective targeting of the GLUT4 gene impairs insulin action in muscle and liver. Nature 2001;409: 729–733
8. He W, Barak Y, Hevener A, et al. Adipose-specific peroxisome proliferator-activated receptor gamma knockout auses insulin resistance in fat and liver but not in muscle. Proc Natl Acad Sci U S A 2003;100: 15712–15717
9. Imai T, Jiang M, Chambon P, Metzger D. Impaired adipogenesis and lipolysis in the mouse upon selective ablation of the retinoid X receptor alpha mediated by a tamoxifen-inducible chimeric Cre recombinase (Cre-ERT2) in adipocytes. Proc Natl Acad Sci U S A 2001; 98:224–228
10. Danielian PS, Muccino D, Rowitch DH, Michael SK, McMahon AP. Modification of gene activity in mouse embryos in utero by a tamoxifen-inducible form of Cre recombinase. Curr Biol 1998;8:1323–1326
11. Elmasri H, Karaaslan C, Teper Y, et al. Fatty acid binding protein 4 is a target of VEGF and a regulator of cell proliferation in endothelial cells. FASEB J 2009;23:3865–3873
12. Fu Y, Luo N, Lopes-Virella MF. Oxidized LDL induces the expression of ALBP/aP2 mRNA and protein in human THP-1 macrophages. J Lipid Res 2000;41:2017–2023
13. Fu Y, Luo N, Lopes-Virella MF, Garvey WT. The adipocyte lipid binding protein (ALBP/aP2) gene facilitates foam cell formation in human THP-1 macrophages. Atherosclerosis 2002;165:259–269
14. Makowski L, Boord JB, Maeda K, et al. Lack of macrophage fatty-acid-binding protein aP2 protects mice deficient in apolipoprotein E against atherosclerosis. Nat Med 2001;7:699–705
15. Ferrell RE, Kimak MA, Lawrence EC, Finegold DN. Candidate gene analysis in primary lymphedema. Lymphat Res Biol 2008;6:69–76
16. Urs S, Harrington A, Liaw L, Small D. Selective expression of an aP2/Fatty Acid Binding Protein 4-Cre transgene in non-adipogenic tissues during embryonic development. Transgenic Res 2006;15:647–653

17. Eguchi J, Wang X, Yu S, et al. Transcriptional control of adipose lipid handling by IRF4. Cell Metab 2011;13:249–259
18. Wang ZV, Deng Y, Wang QA, Sun K, Scherer PE. Identification and characterization of a promoter cassette conferring adipocyte-specific gene expression. Endocrinology 2010;151:2933–2939
19. Soriano P. Generalized lacZ expression with the ROSA26 Cre reporter strain. Nat Genet 1999;21:70–71
20. Brüning JC, Michael MD, Winnay JN, et al. A muscle-specific insulin receptor knockout exhibits features of the metabolic syndrome of NIDDM without altering glucose tolerance. Mol Cell 1998;2:559–569
21. Tomita S, Sinal CJ, Yim SH, Gonzalez FJ. Conditional disruption of the aryl hydrocarbon receptor nuclear translocator (Arnt) gene leads to loss of target gene induction by the aryl hydrocarbon receptor and hypoxia-inducible factor 1alpha. Mol Endocrinol 2000;14:1674–1681
22. Klöting N, Koch L, Wunderlich T, et al. Autocrine IGF-1 action in adipocytes controls systemic IGF-1 concentrations and growth. Diabetes 2008;57:2074–2082
23. Harfe BD, McManus MT, Mansfield JH, Hornstein E, Tabin CJ. The RNaseIII enzyme Dicer is required for morphogenesis but not patterning of the vertebrate limb. Proc Natl Acad Sci U S A 2005;102:10898–10903
24. Cobb J, Dierich A, Huss-Garcia Y, Duboule D. A mouse model for human short-stature syndromes identifies Shox2 as an upstream regulator of Runx2 during long-bone development. Proc Natl Acad Sci U S A 2006;103:4511–4515
25. Larsson NG, Wang J, Wilhelmsson H, et al. Mitochondrial transcription factor A is necessary for mtDNA maintenance and embryogenesis in mice. Nat Genet 1998;18:231–236
26. Jones JR, Barrick C, Kim KA, et al. Deletion of PPARgamma in adipose tissues of mice protects against high fat diet-induced obesity and insulin resistance. Proc Natl Acad Sci U S A 2005;102:6207–6212
27. Blüher M, Michael MD, Peroni OD, et al. Adipose tissue selective insulin receptor knockout protects against obesity and obesity-related glucose intolerance. Dev Cell 2002;3:25–38
28. Lee KY, Gesta S, Boucher J, Wang XL, Kahn CR. The differential role of Hif1β/Arnt and the hypoxic response in adipose function, fibrosis, and inflammation. Cell Metab 2011;14:491–503
29. Vernochet C, Mourier A, Bezy O, et al. Adipose-Specific Deletion of TFAM Increases Mitochondrial Oxidation and Protects Mice against Obesity and Insulin Resistance. Cell Metab 2012;16:765–776
30. Boucher J, Mori MA, Lee KY, et al. Impaired thermogenesis and adipose tissue development in mice with fat-specific disruption of insulin and IGF-1 signalling. Nat Commun 2012;3:902
31. Kleiner S, Mepani RJ, Laznik D, et al. Development of insulin resistance in mice lacking PGC-1α in adipose tissues. Proc Natl Acad Sci U S A 2012;109:9635–9640
32. Owen C, Czopek A, Agouni A, et al. Adipocyte-specific protein tyrosine phosphatase 1B deletion increases lipogenesis, adipocyte cell size and is a minor regulator of glucose homeostasis. PLoS ONE 2012;7:e32700
33. Bettaieb A, Matsuo K, Matsuo I, et al. Adipose-specific deletion of Src homology phosphatase 2 does not significantly alter systemic glucose homeostasis. Metabolism 2011;60:1193–1201
34. Soyal SM, Mukherjee A, Lee KY, et al. Cre-mediated recombination in cell lineages that express the progesterone receptor. Genesis 2005;41:58–66
35. Mudhasani R, Puri V, Hoover K, Czech MP, Imbalzano AN, Jones SN. Dicer is required for the formation of white but not brown adipose tissue. J Cell Physiol 2011;226:1399–1406
36. Jiang C, Qu A, Matsubara T, et al. Disruption of hypoxia-inducible factor 1 in adipocytes improves insulin sensitivity and decreases adiposity in high-fat diet-fed mice. Diabetes 2011;60:2484–2495
37. Imai T, Takakuwa R, Marchand S, et al. Peroxisome proliferator-activated receptor gamma is required in mature white and brown adipocytes for their survival in the mouse. Proc Natl Acad Sci U S A 2004;101:4543–4547
38. Dubois NC, Hofmann D, Kaloulis K, Bishop JM, Trumpp A. Nestin-Cre transgenic mouse line Nes-Cre1 mediates highly efficient Cre/loxP mediated recombination in the nervous system, kidney, and somite-derived tissues. Genesis 2006;44:355–360
39. Yang WJ, Yang DD, Na S, Sandusky GE, Zhang Q, Zhao G. Dicer is required for embryonic angiogenesis during mouse development. J Biol Chem 2005;280:9330–9335
40. Agardh HE, Folkersen L, Ekstrand J, et al. Expression of fatty acid-binding protein 4/aP2 is correlated with plaque instability in carotid atherosclerosis. J Intern Med 2011;269:200–210
41. Vooijs M, Jonkers J, Berns A. A highly efficient ligand-regulated Cre recombinase mouse line shows that LoxP recombination is position dependent. EMBO Rep 2001;2:292–297
42. Mudhasani R, Imbalzano AN, Jones SN. An essential role for Dicer in adipocyte differentiation. J Cell Biochem 2010;110:812–816
43. Shi X, Burkart A, Nicoloro SM, Czech MP, Straubhaar J, Corvera S. Paradoxical effect of mitochondrial respiratory chain impairment on insulin signaling and glucose transport in adipose cells. J Biol Chem 2008;283:30658–30667
44. Silva JP, Köhler M, Graff C, et al. Impaired insulin secretion and beta-cell loss in tissue-specific knockout mice with mitochondrial diabetes. Nat Genet 2000;26:336–340
45. Sterky FH, Lee S, Wibom R, Olson L, Larsson NG. Impaired mitochondrial transport and Parkin-independent degeneration of respiratory chain-deficient dopamine neurons in vivo. Proc Natl Acad Sci U S A 2011;108:12937–12942
46. Wang J, Silva JP, Gustafsson CM, Rustin P, Larsson NG. Increased in vivo apoptosis in cells lacking mitochondrial DNA gene expression. Proc Natl Acad Sci U S A 2001;98:4038–4043
47. Kaestner KH, Christy RJ, Lane MD. Mouse insulin-responsive glucose transporter gene: characterization of the gene and trans-activation by the CCAAT/enhancer binding protein. Proc Natl Acad Sci U S A 1990;87:251–255
48. Tontonoz P, Hu E, Graves RA, Budavari AI, Spiegelman BM. mPPAR gamma 2: tissue-specific regulator of an adipocyte enhancer. Genes Dev 1994;8:1224–1234
49. Alt EU, Senst C, Murthy SN, et al. Aging alters tissue resident mesenchymal stem cell properties. Stem Cell Res (Amst) 2012;8:215–225
50. Serrano R, Villar M, Martínez C, Carrascosa JM, Gallardo N, Andrés A. Differential gene expression of insulin receptor isoforms A and B and insulin receptor substrates 1, 2 and 3 in rat tissues: modulation by aging and differentiation in rat adipose tissue. J Mol Endocrinol 2005;34:153–161
51. Martens K, Bottelbergs A, Baes M. Ectopic recombination in the central and peripheral nervous system by aP2/FABP4-Cre mice: implications for metabolism research. FEBS Lett 2010;584:1054–1058